



# A removable use of FRP for the confinement of heritage masonry columns

Francesco Micelli · Alessio Cascardi  · Maria Antonietta Aiello

Received: 24 July 2023 / Accepted: 5 November 2023 / Published online: 2 December 2023  
© The Author(s) 2023

**Abstract** For masonry structures in historical heritage with architecturally valuable features, such as frescoed surfaces, the application of structural reinforcement techniques appears to be very complex due to the requirements of removability and limited invasiveness. This is valid with reference to both traditional techniques and modern techniques, such as the external reinforcement with fibre-reinforced composite materials. In this scenario, the use of *fibers reinforced polymers* (FRPs) is drastically forbidden due to the use of epoxy-based matrix, which does not allow the removal of the intervention without damage of the substrate, even if the mechanical effectiveness of this system has been largely tested and proved. In fact, the reversibility is one of the most relevant aspects in the field of Heritage engineering. Thus, many efforts need to be spent in order to meet possible solutions, able to mitigate the risk, especially against seismic forces and other natural risks, while ensuring the conservation of the built heritage. This

experimental research, which follows a first study on a smaller scale, aims to answer the question: how could a masonry column with frescoes and valuable surfaces be strengthened or repaired in a completely reversible manner?. Two strengthening methods were studied and are proposed herein by assuring the removability of the FRP-confinement of masonry columns. The first technique consists of a liquid adhesion inhibitor applied by brush before the hand lay-up installation of the FRP. The second is set by the interposition of a *Mylar*<sup>TM</sup> layer between the substrate and the FRP jacket. Uniaxial compression tests were performed in order to demonstrate the efficacy of the new strengthening techniques in increasing the axial strength (+ 39% and + 27% on average for the tuff- and limestone-based masonry, respectively) and displacement capacity (+ 32% and + 171% on average for the tuff- and limestone-based masonry, respectively) with respect to un-confined columns. Masonry columns FRP-confined with traditional wet lay-up were also tested for direct comparison. At a later moment, the FRP-jacket was removed to observe the substrate, which has been found effectively preserved from the adhesive, without any discoloration. The experimental results are extensively shown and discussed in the paper.

---

F. Micelli · M. A. Aiello  
Department of Innovation Engineering, University of Salento, 73100 Lecce, Italy  
e-mail: francesco.micelli@unisalento.it

M. A. Aiello  
e-mail: antonietta.aiello@unisalento.it

A. Cascardi (✉)  
Department of Civil Engineering, University of Calabria, 87036 Cosenza, Italy  
e-mail: alessio.cascardi@unical.it

**Keywords** Heritage · Masonry · FRPs · Confinement · Testing · Removability



## 1 Introduction

A large part of the existing masonry buildings, many of which are recognized as cultural Heritage, require reinforcement or structural rehabilitation for protection against catastrophic events, such as earthquakes, floods, explosions, overloads, environmental degradation, etc. The recent seismic events have demonstrated, once again, that masonry is prone to brittle collapses due to cyclic in-plane forces, and this often causes the loss of valuable heritage [1]. In particular, in Italy about the 57% of the residential built heritage consists of masonry, while 56% of this heritage is dated back '70 [2]. In addition, the high seismicity of the national territory increases the risk; in fact, the most recent regulations [3] have acknowledged the entire national territory as exposed to seismic hazard. When dealing with cultural heritage, the choice of the proper intervention is hard to achieve since it should balance the adherence to safety standards and the preservation of the historic architectural value. In this perspective, the reversibility or, at least, the maximum removability is mandatory [4–11]. In addition, the proposed techniques could be easily utilized as short-term countermeasure in the post-earthquake stage (e.g. in the presence of frescos as shown in Fig. 1). In fact,



**Fig. 1** Example of a fresco on a column into the Cathedral of Santa Maria Assunta in Nardò (Italy)

after the main seismic shock, even if the building did not collapse, cracks and damages might be found, which make the structure extremely vulnerable when aftershock seismic activity will take place. In this timeframe a fast and removable strengthening technique is the only solution that could preserve the integrity of the columns and its historical value at the same time.

The reversibility should be intended as a target that should be respectful of criteria and recommendations that regulated by national legislations and international guidelines. According to [10], the removal or alteration of any historic material or distinctive architectural features should be avoided whenever possible. Moreover, current measures may be removed and replaced with more suitable future measures when new knowledge is acquired. Where they are not completely reversible, interventions should not limit further interventions. A distinctive historic feature is reported in [11], or rather, the removal or alteration of any historic material or distinctive architectural features should be avoided wherever possible. In other words, where possible, any measures adopted should be removable and replaced with more suitable measures required. A reversible intervention is defined in [12] as the intervention which integrates the resistant elements and/or conditions the stresses without permanently transforming the original structure. According to this explanation, in the same document, the use of FRPs is assumed to be “not full-reversible”; [13–24]. In fact, there is a remarkable increase in the mechanical performance for continuous FRP-confined masonry. For example, calcarenite stone was experienced in [25] with adverse effects studied in the performed experiments, such as the water/moisture influence. The FRP-jacket led to compressive strength increase between 2.5 and 2.75 with respect to the unconfined natural rock. Besides, the ultimate strain increases up to 20 times when strengthened using glass fiber fabrics. Further results of an experimental test on FRP-confined tuff-based masonry, subjected to static axial load, is reported in [22]. Both regular and irregular (with cavity) arrangements for the masonry columns were considered. The axial strength increased up to 85% and 112% for the regular and irregular masonry, respectively. Also, the post-elastic behavior benefited of axial ductility gain. Carbon-based FRP-jacket proved to be effective in reliably increasing the axial strength of concrete block-based

masonry, [26]. Noticeable was also the softening trend in the post peak behavior demonstrating a residual axial strength after the crush and a significant axial ductility.

Moreover, the theoretical aspect of the FRP-confinement of masonry columns is a focusing issue. Masonry confinement theory is commonly derived from concrete confinement. A masonry-targeted approach is proposed in [27]. The model was based on the masonry density or alternatively on the properties of the brick and mortar, as well as on the mechanical properties of the composite. Furthermore, the influence given by cross sectional shape and effective strain level in FRP wrapping. The model predictability was tested at different scale levels. It was found that the lower FRP efficiency was found for real scale masonry based on available experimental results. A different expression was proposed for the prediction of compressive strength of masonry prisms with the loading axis inclined to bed joint in [28]. The investigations highlighted the importance of assessing a parameter able to take into account the inclination of the mortar joint. These and many other studies demonstrated that the theoretical prediction of the behavior of an axial FRP-confined masonry column involves assessing how the column will respond to axial loads and confinement provided by FRP-materials. This prediction is typically made using structural engineering principles and mathematical models. The first step is to gather information on the properties of the materials involved. This includes the strength of the masonry and the mechanical properties of the FRP materials. The masonry is typically modeled as a core and an external FRP layer. The interaction between the core and the FRP is considered. With the confinement effect considered, the axial load-carrying capacity of the confined masonry column can be also predicted. This is typically done using equilibrium equations and strength criteria. The goal is to find the maximum axial load that the column can withstand without failure. The column's ductility, which refers to its ability to deform and absorb energy before failure, is another important factor. Ductility can be assessed using displacement-based criteria, such as drift limits, which are often defined by building codes and seismic design requirements.

The present research aims to provide a contribution in the field of FRP-confinement of masonry columns when the reversibility of the external strengthening is mandatory. The present experimental investigation is the direct continuation of a previous (and preliminary)

study concerning stone blocks [29]. The mechanical tests on half-scale masonry columns that are shown and discussed herein, definitely demonstrate the validity of the proposal and the grade of reversibility of the different techniques, without losing the mechanical upgrade of the external confinement in terms of both axial loads bearing capacity and ductility. First of all, a solid and level foundation to build the column on was ensured by adopting a concrete pad. Manufacturing started by laying the first course of bricks or blocks and, consequently, applying a bed of mortar on the foundation and then setting the first row of bricks or blocks, making sure they were level and plumb by using a level and a string line to check for accuracy. It continued adding courses of bricks or blocks, applying mortar between each layer. Offsetting the joints between courses to increase the stability of the column was imposed. More details on the geometrical dimensions of the sample are provided in the next section. After that, the curing started. The mortar was allowed to cure for at least 28 days before continuing with the test.

In particular, two removable FRP-based confinement techniques are proposed:

1. *Interposition of a Separating Film (ISF)* It consists in introducing a film between the column and the FRP-jacket. This prevents the thermosetting matrix from impregnating the substrate, thus avoiding the irreversible permanent bond, which generally characterizes confinement with FRP wrapping. This approach does not prejudice the mechanical benefits of external confinement since the confining pressure can be applied by simple contact between the core and the jacket while perfect bond is not necessary. In fact, the FRP is passively activated by the lateral deformation of the core material, which generates a state of traction in the FRP coating in the circumferential direction. In this sense, the contact between the substrate and the reinforcement is theoretically ensured up to the breaking of the fiber or the loss of adhesion in the overlapping region. The film, interposed between the original substrate and the reinforcing jacket should have several features for a successful application. In particular, it should have *negligible roughness* to limit the friction between the FRP and the masonry substrate, thus facilitating a possible future removal; *flexibility*

(i.e. low stiffness) to make installation quick and easy; resistance to heat produced by the exothermic cross-linking reaction of the epoxy matrix, and possible *low cost*. Therefore, the choice falls on using a Mylar™ film as a separation impermeable layer. Mylar™ is the trade name used to indicate a polyethylene terephthalate (PET) film characterized by a thickness of about 0.03 mm, negligible surface roughness and non-adhesive detaching properties.

2. *Liquid Adhesion Inhibitor* (LAI) It consists in previously treating the surface of the masonry with an adhesion inhibiting liquid. The goal is to create a protective and transparent layer that avoids the bond between the FRP and the masonry. To ensure the effectiveness of the technique, an appropriate liquid release agent must be used, able to allow the detachment of the resin and therefore, the future removal of the reinforcement without physical and chromatic alterations of the substrate. Based on the effectiveness demonstrated in the previous study [29], the liquid used is composed of two parts of a silane-based waterproofing commercial solution and one part of a release agent used in composites industry. The waterproofing solution (*MAPEI Antipluviol W*) is a colorless water-repellent impregnating agent based on silanes and siloxanes in aqueous emulsion; while as a release agent, a film release agent in aqueous solution PVA (Poly Vinyl Alcohol) called Z-16 was used. The identification codes (ID) for the used products are: A for Antipluviol W, and Z for the film release agent Z-16. It follows that the composition of the liquid inhibiting adhesion is indicated by the ID: AAZ. The use of the aforementioned materials is due to the fact that the chemical adhesion, when using epoxy resin, is developed by means of hydrogen bonds, to prevent which, the liquid release agents used must possess water-repellent characteristics. Furthermore, these kinds of materials are also used to protect the masonry substrate from atmospheric agents.

## 2 Experimental program

The experimental program included a total of 16 samples in the form of half-scale masonry columns. The main purposes of the mechanical tests were to

assess the strengthening effectiveness of the non-adhesive FRP-confinement. At the same time, the second purpose was to check the degree of reversibility of the confinement with C-FRP (*Carbon-Fiber Reinforced Polymer*) by varying both the substrate material and the reinforcement application technique. In all cases, the columns were wrapped with a unidirectional carbon fiber sheet applied in a single layer using two-component epoxy-based resin. In particular, 8 specimens were made by blocks of Neapolitan tuff (hereinafter named “NAP”) and 8 specimens by blocks of Lecce stone (hereinafter named “PL”). Lecce stone is a soft limestone dating from the Miocene period, settled in the sea and subsequently emerged. Neapolitan yellow tuff was formed from whitish-colored volcanic ash, which settled in the sea and subsequently emerged as a result of tectonic pressures, dated between 35,000 and 10,500 years ago. Two very porous stones, typically used in heritage masonry, were specifically chosen, in order to better evaluate the effectiveness, in terms of reversibility, of the confinement techniques proposed herein. The material properties of the adopted masonry units and mortar for the construction the columns are reported in Table 1 with their CoVs (*Coefficient of Variations*).

Concerning the first set of 8 NAP-specimens, two (follow labeled as “NAP-FRP-01” and “NAP-FRP-02”) were fully wrapped with C-FRP jacket by using the wet lay-up technique; in this case an epoxy primer was preliminary applied on the column’s substrate, then the first layer of resin, the Carbon sheet and the second resin layer. Two specimens (the nomenclature adopted is “NAP-MYL-01” and “NAP-MYL-02”) were first coated with a Mylar™ film, according to the ISF technique, and then they were wrapped with C-FRP by the wet lay-up technique, upon the Mylar™ skin. Two specimens were impregnated with the *adhesion-inhibiting liquid* AAZ, according to the LAI technique, and then confined using C-FRP sheet (identified as “NAP-LIQ-01” and “NAP-LIQ-02”); lastly, two specimens were left without external reinforcement, i.e. not confined, so as to be taken as reference samples for the comparison of the results (called “NAP-URM-01” and “NAP-URM-02”). The above-mentioned NAP-samples were made of squared blocks in Neapolitan tuff having dimensions  $55 \times 120 \times 250 \text{ mm}^3$ ; the joints were about 10 mm thick, and they were made of a lime-based mortar,



**Table 1** Mechanical properties of the masonry's constituents

Property	Unit	NAP	PL	Mortar
Compressive strength (CoV)	MPa	5.22 (0.5)	12.43 (1.1)	10.41 (1.5)
Bending/tensile strength (CoV)	MPa	–	–	1.68 (0.6)
Elastic Modulus (CoV)	GPa	0.9 (0.06)	1.6 (0.05)	9.7 (1.1)

according to the traditional construction techniques used in heritage buildings. The resulting half-scale columns had a height— $h$ —of 600 mm, corresponding to nine courses of blocks, and a square section of— $axb$ —size equal to  $250 \times 250 \text{ mm}^2$ . Moreover, the corners were rounded with a radius of curvature— $r_c$ —equal to 20 mm in order to avoid a “*knife effect*” that could lead to a premature failure of the carbon fibers due to stress concentration at the corners. Figure 2 shows the dimensions and the stratigraphy of the various types of reinforcement adopted for the NAP specimens.

Similarly, as regards the 8 PL-series, two specimens were “traditionally” confined with C-FRP (i.e. “PL-FRP-01” and “PL-FRP-02”) by using the manual wet lay-up. Two specimens were first wrapped with aMylar<sup>TM</sup> film, according to the ISF technique, and then they were wrapped with C-FRP (namely “PL-MYL-01” and “PL-MYL-02”); two were impregnated with the adhesion-inhibiting AAZ liquid, according to the LAI technique, and then confined using C-FRP (namely “PL-LIQ-01” and “PL-LIQ-02”). Lastly, two reference samples were left unconfined for the comparison of the results (namely “PL-URM-01” and “PL-URM-02”). The PL samples were made using squared blocks of Lecce stone  $55 \times 120 \times 250 \text{ mm}^3$ . For the joints, about 10 mm thick, the same lime-based mortar was used, according to the traditional construction techniques used in heritage buildings. The resulting half-scale columns had a height –  $h$ —of 660 mm, corresponding to ten courses of blocks, and a square section of— $axb$ —size equal to  $250 \times 250 \text{ mm}^2$ . The corners have been rounded to ensure a  $r_c$  equal to 20 mm. Figure 3 shows the dimensions and the stratigraphy of the various types of reinforcement adopted for the case of the PL-specimens.

In all confined specimens, a single unidirectional CFRP sheet was used as external jacket, by placing the fibers in the  $90^\circ$  direction respect to the principal

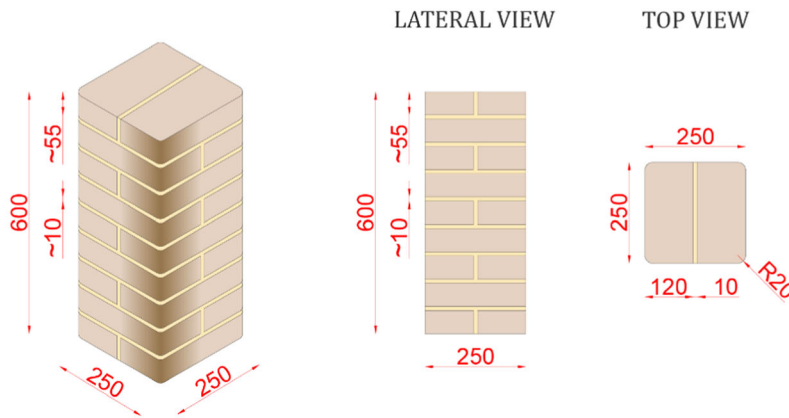
(vertical) axis of the columns. The overlap region is shown in Figs. 2 and 3 fixed equal to one side of the cross-section or rather 250mm.

Each group of samples was tested under axial compression until failure and the ultimate strength and ductility values of the confined specimens were compared with those obtained for the reference (non-confined) specimens. In a later moment, after the tests, the C-FRP jacket was carefully removed in order to evaluate the reversibility of the innovative confinement techniques adopted (LAI and ISF), through a visual comparison of the state of the substrate upon removal with specimens classically wrapped (NAP-FRP and PL-FRP).

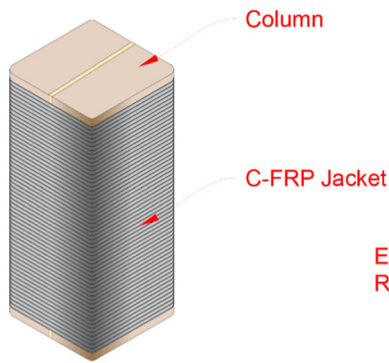
## 2.1 Test set-up

The columns were all subjected to axial compression tests into a closed and rigid steel frame. At the base of the sample a rigid square steel plate with a thickness of 30 mm was placed and other plates with a thickness of 25 mm were placed on the top of the sample so as to make it rigidly contrasted within the frame and uniformly loaded at the end sections. The load was applied by means of a 250-ton hydraulic jack, which reacts against the aforementioned steel frame, and is operated by means of a manual hydraulic pump. So, the load was hand-imposed taking care to keep a load-rate uniform and slow as much as possible. In all tests, two displacement transducers (LVDTs) with 100 mm measure length were used to record the shortening of the column in the longitudinal direction. In detail, the two LVDTs were located at opposite corners of the steel plate at the head of the specimen, in order to average the recorded results, in order to consider possible effects due to accidental eccentricities and measure the shortening induced by the axial load. The applied load was measured by means of a load cell with a capacity of 30-ton. Load, deformations, and displacements values were recorded in real time by an

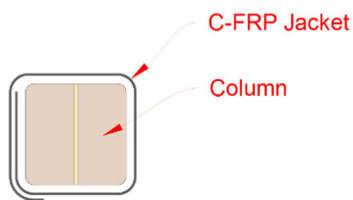
**NAP-URM-01 / NAP-URM-02**



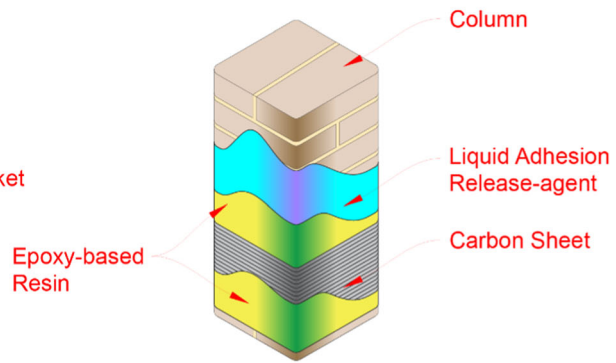
**NAP-FRP-01 / NAP-FRP-02**



TOP VIEW



**NAP-LIQ-01 / NAP-LIQ-02**



**NAP-MYL-01 / NAP-MYL-02**

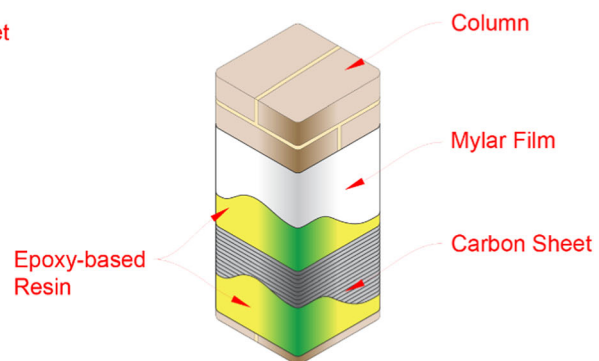


**Fig. 2** Specimen's description: NAP-series (dimensions in mm)

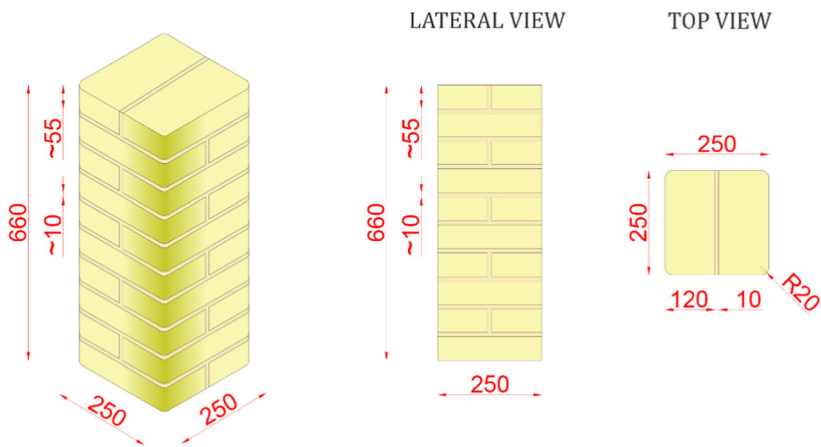
electronic data acquisition system. All tests were conducted under the same (standard) temperature and humidity conditions. Figure 4 shows the photo of the test set-up described above.

**2.2 Removability check**

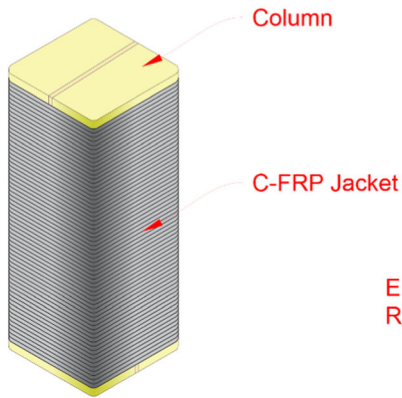
Once the axial compression tests have been ended and the columns were unloaded, the C-FRP jacket was



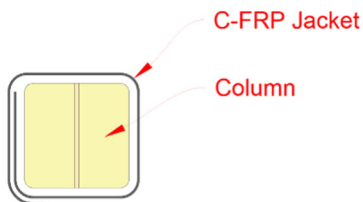
**PL-URM-01 / PL-URM-02**



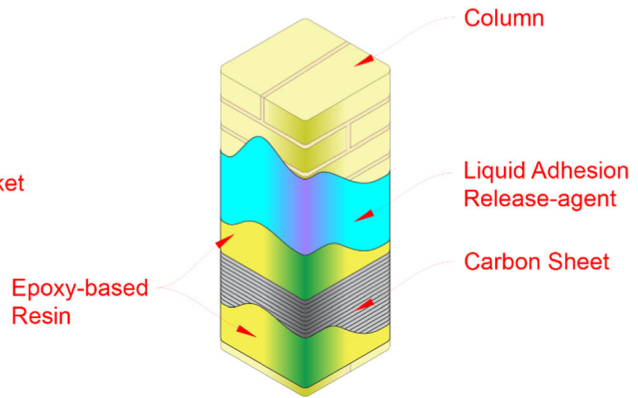
**PL-FRP-01 / PL-FRP-02**



TOP VIEW



**PL-LIQ-01 / PL-LIQ-02**



**PL-MYL-01 / PL-MYL-02**

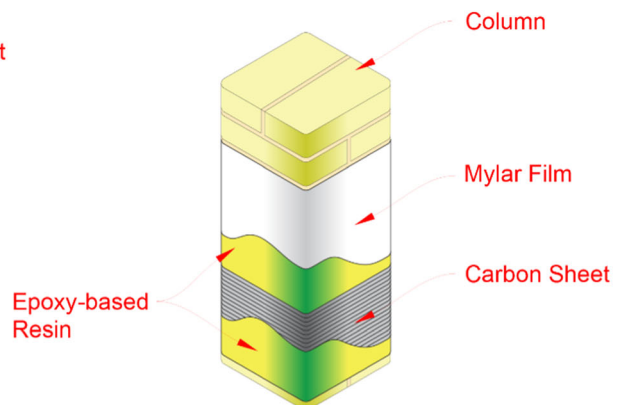


**Fig. 3** Specimen's description: PL-series (dimensions in mm)

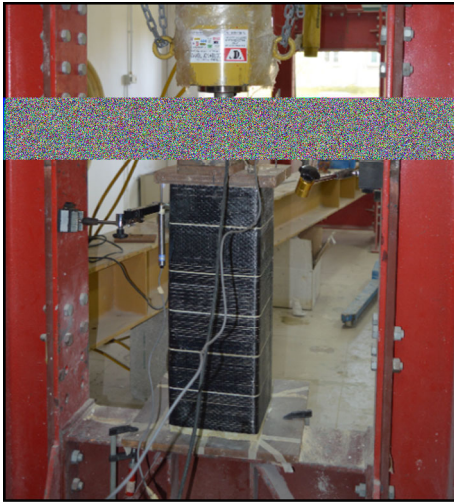


**Fig. 4** Test set-up

removed from each specimen, operating a vertical cut in the composite layer. This allowed to assess the degree of removability or even reversibility of the C-FRP confinement installed with the three different techniques as reported in Fig. 7. When the reinforcement is “traditionally” applied to the masonry, using the manual wet lay-up technique, it was not possible to easily remove the C-FRP jacket because of the penetration of the adhesive inside the masonry substrate. In this case the removal was possible only by a complete detachment of the penetrated masonry. From the observation of the reinforcement, in fact, very deep portions of the masonry substrate appear fully bonded to the C-FRP jacket (Fig. 5a and d); the specimens, on the other hand, remain severely altered and scarred. So, as expected, in the case of manual wet lay-up the external C-FRP reinforcement should be considered not removable. By removing the C-FRP outer jacket from the LIQ-series specimens, acceptable removability is achieved (see Fig. 5b and e). Definitely, the application of an adhesion-inhibiting liquid before applying the reinforcement allows for easy removal of the C-FRP jacket. However, the LAI technique cannot be considered fully reversible. In fact, from the observation of the removed jackets, thin portions of the substrate linked to the FRP are found, with a consequent small alteration of the surface of the sample. In the case of Lecce stone, the alteration is not only physical but also chromatic. Another observation derives from the comparison between the jacket removed from the PL specimens and the one removed

from the NAP specimens. In fact, in the first case the portions of substrate which remain bound to the jacket are minimal and somewhat superficial, while in the case of NAP specimen’s deeper detachments occur. This is attributable to the higher porosity of the Neapolitan tuff compared to the Lecce stone, also by considering the low viscosity of the adhesion inhibiting liquid used. These factors allowed a small penetration of the release agent into the masonry without forming a film that could be able to separate the epoxy adhesive from the substrate.

Finally, as regards the MYL series specimens, it was possible to completely remove the C-FRP jacket, without appreciating any alteration of the specimens, as can be seen from Fig. 7c and f, related to the NAP and PL specimens, respectively. By coating the columns with *Mylar*<sup>TM</sup> sheets before applying the resin, the C-FRP jacket forms a non-adhesive casing that can be easily and completely removed without any alteration of the inner masonry core. The substrate remains isolated and does not undergo any aesthetic or chromatic alteration. It follows that the ISF reinforcement technique is not only removable but also reversible, as it allows the reinforcement to be removed without leaving traces, as required by the ISCARSAH’s principles [10], as well as in [12].

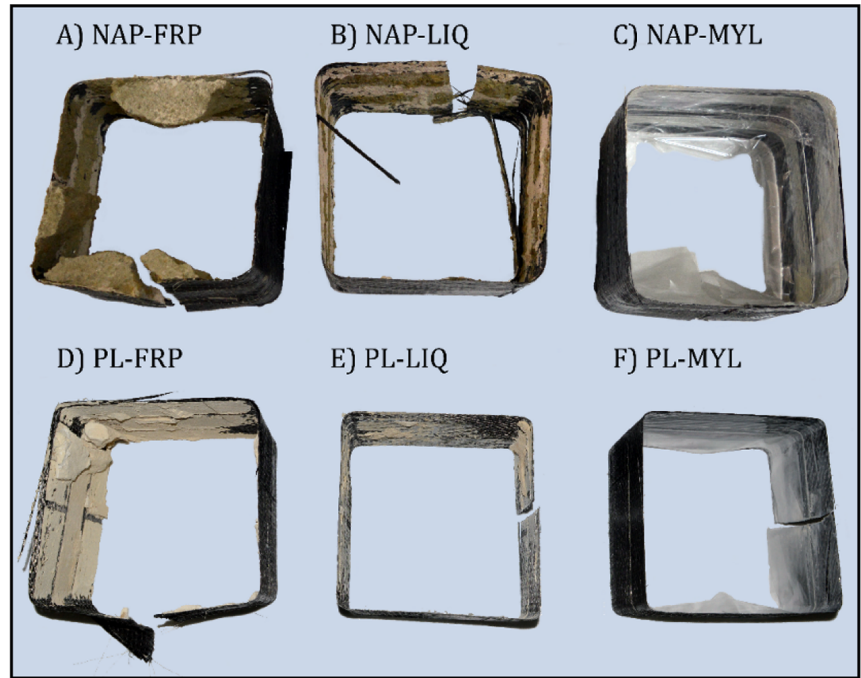
### 3 Results and discussion

#### 3.1 Compression tests

The results in terms of axial stress–strain are reported in Fig. 6a and b, for NAP and PL series, respectively. The first was calculated as the measured load level (load cell) divided by the cross-section of the sample; while the latter was assumed equal to the measured longitudinal shortening (averaged LVDTs) divided by the initial un-load height of the column itself. Referring to specimens of the NAP-URM and PL-URM series the tests led to similar results for the two repetition specimens made with the same stone. A typical brittle behavior has been observed, with a sudden drop in resistance in correspondence with the crushing of the column. The PL series specimens exhibited higher stiffness and higher strength, as expected by considering the higher density of this stone. The beneficial effect of the confinement is evident. In fact, an increase in ultimate strength has



**Fig. 5** Removability comparison: **a** FRP-jackets, **b** NAP-LIQ, **c** PL-LIQ, **d** NAP-MYL and **e** PL-MYL



a)



b)



c)



d)



e)

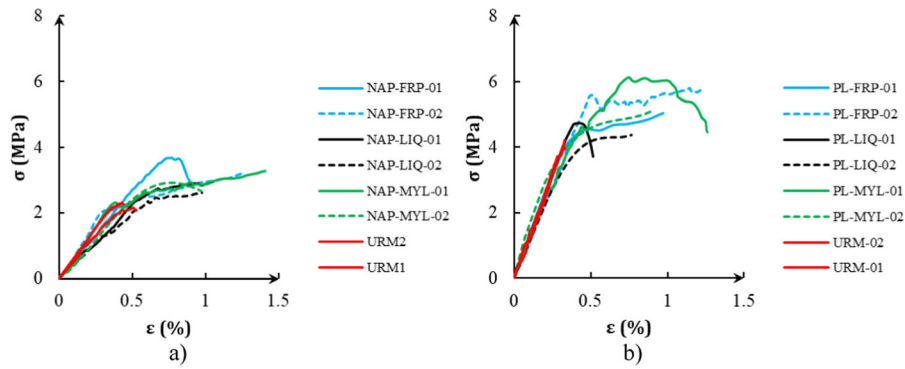


**Fig. 6** Test results in forms of tension vs axial strain curves: **a** NAP and **b** PL series



**Fig. 7** Crushing typically observed after the C-FRP jacket removal



**Fig. 9** arching effect in the cross-section of the column

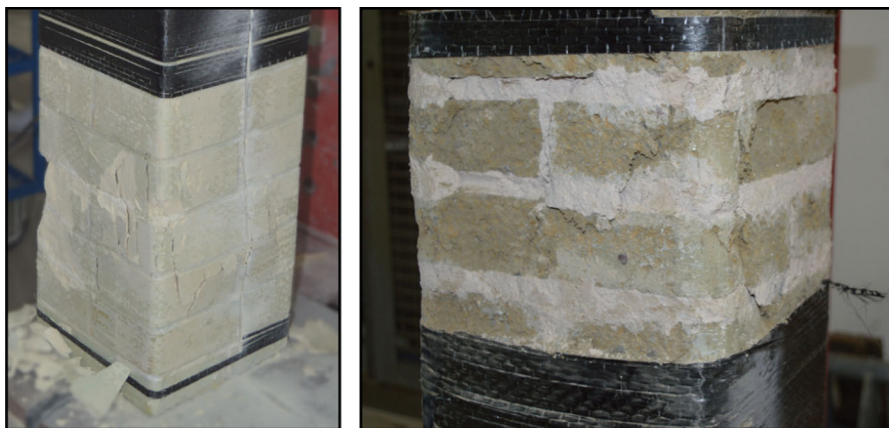


**Fig. 8** Local detachments typically observed after the C-FRP jacket removal

been registered in all cases, as well as a more extensive post peak branch, which denotes a more ductile response of the confined specimens. For specimens of

each pair (NAP and PL) the results are quite comparable, even if some differences are visible. The two PL-MYL columns had a different behaviour in the

second branch of the curve, when confinement becomes active. One specimen exhibited a pronounced hardening behaviour (PL-MYL-01), with a peak load and a softening final branch, while in the second repetition the slope of the hardening branch was lower, without softening. Differences are visible also for PL-FRP and NAP-FRP repetitions, where one of the two specimens had a higher strength respect to the correspondent second column. All these differences can be considered within the experimental error since the materials tested are natural and brittle, therefore the presence of invisible defects may provoke differences in the cracking formation and development, with a different response in the cracked stage, when the external confinement is more active. In case of NAP series, the sample NAP-FRP-01 exhibits a softening trend in the post peak branch, while the alter ego a hardening behavior as just said this difference may be attributable to the unpredictable cracking evolution of the masonry core inside the CFRP jacket. By comparing all the curves in Fig. 6 it can be observed that the interposition of the *Mylar*<sup>TM</sup> sheet between the C-FRP jacket and the masonry does not compromise the effectiveness of confinement, which produces an increase in strength and ductility of the columns. In this case, two specimens show a softening trend of the post peak branch, NAP-MYL-02 and PL-MYL-01.

Also in this case, LIQ-method, the effectiveness of the confinement and the repeatability of the results for the specimens of each pair (NAP and PL) are both evident. The post-peak branch exhibits a hardening trend in all cases, except in the case of the PL-LIQ-01 specimen.

The rather poor mechanical characteristics of the tuff and the considerable variability of the local resistance have led to a failure mode characterized by several vertical cracks affecting different blocks of the samples. On the contrary, the higher quality of the Lecce stone specimens has generally led to a failure mode characterized by a main vertical crack that crosses the blocks on the four faces of the sample, a transverse expansion in the medium–high area of the column and consequent local detachments of the masonry prisms between the cracks, leaving almost all of the blocks mostly intact. Once the C-FRP layer was removed, it was possible to assess the surface condition of the masonry columns after testing. First of all, they all highlighted similar modes of crisis. Fragments

of stone were detached from the column well before the fibers were completely broken by tension; this highlight how the carbon fibers prove to be highly performing when applied for the external confinement by continuous wrapping of the masonry columns, being the ultimate deformation of these fibers greater an order of magnitude than that of the masonry. It was possible to observe in some cases, that the fibers broke at the corners (even if rounded), due to the concentration of the stress at these zones. To sum up, the columns, “stripped” of the reinforcement, showed:

- Vertical cracks, affecting both blocks and mortar joints (see Fig. 7)
- Local detachments (see Fig. 8).

The effectiveness of confinement is evident if the cross section of the confined sample is observed. This section is always cracked according to the typical “arching” shape, as can be seen from Fig. 9. Basically, the cracks follow parabolic branches for the establishment of an “arc effect” dependent on the radius of curvature with which are the vertices of the section have been rounded; in this way the effective confined masonry area emerges, that is the confined core typical of rectangular sections confined by an external wrapping. The central regions far from the corners suffer extensive cracking due to the lack of full confinement.

### 3.2 Mechanical performances

The results recorded during the uniaxial compression tests on the samples confined with the C-FRP system, applied with different techniques, aimed at proving the full removability, are reported and discussed, first of all, in relation to the mechanical upgrade. The efficacy of the confinement has been evaluated both in terms of strength and ductility in comparison with the reference samples (i.e. not confined). The results are reported in Table 2 for the NAP specimens and in Table 3 for the PL specimens. In particular the Tables report:

- the peak stress corresponding to a significant change in the slope behavior;
- the strength corresponding to the maximum registered axial stress (equal to the peak stress in case of softening post peak behavior);
- the ultimate axial strain corresponding to the maximum stress;

**Table 2** Efficacy of confinement of NAP specimens, quantified both in terms of strength and in terms of mean ductility of the confined specimens in comparison with the corresponding mean values of the unconfined specimens

Test	Peak Stress	Strength	Ultimate axial strain	Peak axial strain	Elastic Modulus	Ductility ( $\epsilon_u - \epsilon_p$ )/ $\epsilon_p$	$f_{cm}/f_m$	$\mu_{cm}/\mu_m$					
#	Label	$f_p$ (MPa)	$f_m$ (MPa)	$\epsilon_u$ (%)	$\epsilon_p$ (%)	$E$ (MPa)	$\mu$ (%)						
1	NAP-URM-01	2.32	2.32	2.23	0.44	0.43	615.74	3	4	–	–	–	–
2	NAP-URM-02	2.15	2.15		0.53	0.51	533.31	4		–		–	
3	NAP-FRP-01	3.67	3.67	3.43	0.89	0.77	530.36	16	153	1.64	1.54	4	41
4	NAP-FRP-02	2.07	3.19		1.25	0.32	644.46	291		1.43			77
5	NAP-LIQ-01	2.46	2.95	2.79	1.05	0.67	426.14	56	52	1.32	1.25	15	14
6	NAP-LIQ-02	2.47	2.63		0.98	0.66	409.21	48		1.18			13
7	NAP-MYL-01	2.31	3.29	3.10	1.41	0.39	565.19	261	155	1.47	1.39	69	41

- the peak axial strain corresponding to the peak stress;
- the elastic modulus corresponding to the secant modulus between the 5% and 45% of the peak stress;
- the ductility in percentage according to the scatter between the elastic and ultimate axial strain;
- the ratio in term of strength between the confined and un-confined samples;
- the ratio in term of ductility between the confined and un-confined samples;

As can be seen, values of the confined to non-confined strength ratio are ranging between 1.18 and 1.64, for the Neapolitan tuff, while values between

1.07 and 1.50, are found for the PL. Consequently, the confinement was effective, even if with a certain variability, in terms of resistance, in all cases and regardless of the technique utilized. It should be noted that the confinement system with C-FRP adherent to the substrate offers the highest contribution in terms of resistance in the case of NAP specimens. In this case the masonry is of poorer quality, more porous, and an increase up to 64% has been obtained in terms of compression strength for the sample NAP-FRP-01. The minimum mechanical upgrade was recorded for the confinement of the PL-LIQ-02 sample, which nonetheless shows resistance value higher than those of the the un-confined reference sample. This can be attributable also to the evolution of damage during the

**Table 3** Effectiveness of the confinement of the PL specimens, quantified both in terms of resistance and in terms of average ductility of the confined samples in comparison with the corresponding average values of the non-confined samples

Test	Peak Stress	Strength	Ultimate axial strain	Peak axial strain	Elastic Modulus	Ductility ( $\epsilon_u - \epsilon_p$ )/ $\epsilon_p$	$f_{cm}/f_m$	$\mu_{cm}/\mu_m$					
#	Label	$f_p$ (MPa)	$f_m$ (MPa)	$\epsilon_u$ (%)	$\epsilon_p$ (%)	$E$ (MPa)	$\mu$ (%)						
1	PL-URM-01	4.21	4.21	4.10	0.33	0.33	1168.8	0.0	0.7	–	–	–	–
2	PL-URM-02	3.98	3.98		0.33	0.32	1294.2	1.5		–		–	
3	PL-FRP-01	4.28	5.05	5.43	0.97	0.38	1303.2	155	150	1.23	1.33	208	201
4	PL-FRP-02	5.59	5.81		1.24	0.51	1103.3	144		1.42			194
5	PL-LIQ-01	4.71	4.71	4.54	0.51	0.39	1237.4	30	58	1.15	1.11	41	78
6	PL-LIQ-02	3.89	4.38		0.77	0.41	1102.5	85		1.07			114
7	PL-MYL-01	6.12	6.12	5.61	1.26	0.54	1166.7	133	175	1.49	1.37	179	235
8	PL-MYL-02	3.62	5.11		0.90	0.28	1570.2	217		1.25			292

test, since the sample reached a first local compression crush at an angle of the specimen. For the NAP specimens, the confined to non-confined ductility ratio varies between 4 and 77, while for the PL specimens it varies between 41 and 292. In all cases, being this ratio greater than one, it highlights an increase in ductility of the sample offered from confinement. The minimum contribution due to the NAP-FRP-01 sample is attributable to the softening trend of the post peak branch, so that once the peak stress was reached, the stress suddenly drops, which did not allow to exploit any significant ductility reserve of the sample. On the contrary, the development of the post peak branch with a hardening trend, in the case of the PL-MYL-02 sample, made it possible to reach a high value of ultimate deformation, if compared with the peak deformation, determining the maximum value of the ductility ratio between confined and unconfined samples.

As regards the initial elastic modulus, with reference to Table 2, the confined Neapolitan tuff masonry recorded an average value of 507 MPa with a dispersion of 18%; value similar to that of unconfined masonry equal to 574 MPa  $\pm$  10%. Similarly, with reference to Table 3, the confined Lecce stone masonry recorded an average value of 1247 MPa with a dispersion of 14%; also in this case, similar to that of the non-confined masonry of reference equal to 1231 MPa  $\pm$  7%.

The CNR-DT200 design code provides guidelines for the design of FRP confinement for masonry columns, [30]. The compressive strength of the FRP-confined column subjected to a lateral confining pressure,  $f_l$ , is calculated as follow:

$$f_{mc} = f_m + k x f_{l,eff}$$

where  $f_m$  is the compressive strength of the unconfined masonry,  $k'$  is a non-dimensional coefficient, and  $f_{l,eff}$  represents the effective confining pressure. In particular:

$$k' = \frac{g_m}{1000} \quad \text{with } g_m \text{ the masonry mass-density expressed as kg/m}^3$$

$$f_{l,eff} = k_H x f_l \quad \text{with } k_H \text{ the horizontal coefficient of efficiency.}$$

$k_H = \frac{1-(b'^2+d'^2)}{3A_m}$  with  $A_m$  cross-sectional area of the column and  $b$  /  $d$  sides of the prismatic cross-section curtailed by twice the radius of curvature of the edges

$f_l = \frac{2x E_f \varepsilon_f t_f}{D}$  with  $E_f$ ,  $\varepsilon_f$  and  $t_f$  the young's modulus, the maximum elongation and the thickness of the FRP respectively and  $D$  the diagonal of the prismatic cross-section

The results of the CNR DT200 based prediction are reported in Table 4 demonstrating the validity of existing models for the herein proposed removable FRP-confinement techniques.

## 4 Conclusions

In this experimental study different FRP-confinement techniques have been presented and tested, by regarding the removability and reversibility, in relationship to the importance of the architectural and aesthetic value of the column. A total reversibility of the retrofitting process is typically a goal difficult to achieve if it is evaluated as the future possibility of totally restoring the initial conditions. However, in this study it is shown that it is possible to achieve important results in this sense if the choices fall to a proper technique. The choice between traditional and innovative intervention techniques should therefore be made in relation to the specific case, always preferring less invasive and more compatible interventions with the values of the heritage, while ensuring safety and durable conservation. This research investigated the reversibility of new engineering solutions adopted for the confinement of masonry columns with C-FRP composites, as an alternative to the manual wet lay-up confinement that requires the direct impregnation of the masonry with the epoxy resin. The proposed solutions consist of the LAI (*Liquid Adhesion Inhibitor*) technique and the ISF (*Interposition of a Separating Film*) technique. The first one prevents the impregnation of the masonry by the resin, by applying a liquid that inhibits adhesion with the function of release agent; this liquid should create a surface patina that allows to inhibit the adhesion of the resin to the substrate. The second allows to physically separate the masonry from the FRP reinforcement, by wrapping the



**Table 4** Prediction of the compressive strength of the confined columns according to the CNR DT200, [30]

Label	$g_m$ (kg/m <sup>3</sup> )	$k'(-)$	$k_H$ (-)	$E_f$ (GPa) (-)	$\varepsilon_f$	$t_f$ (mm)	$f_l$ (MPa)	$f_{l\text{eff}}$ (MPa)	$f_m$ (MPa)	$f_{mc\text{—}theo}$ (MPa)	$f_{mc\text{—}exp}$ (MPa)	$exp/theo$ (-)
NAP-FRP-01	1100	1.1	0.53	210	0.01	0.167	0.79	0.42	2.24	3.39	3.67	1.08
NAP-FRP-02	1100	1.1	0.53	210	0.01	0.167	0.79	0.42	2.24	3.39	3.19	0.94
NAP-LIQ-01	1100	1.1	0.53	210	0.01	0.167	0.79	0.42	2.24	3.39	2.95	0.87
NAP-LIQ-02	1100	1.1	0.53	210	0.01	0.167	0.79	0.42	2.24	3.39	2.63	0.78
NAP-MYL-01	1100	1.1	0.53	210	0.01	0.167	0.79	0.42	2.24	3.39	3.29	0.97
NAP-MYL-02	1100	1.1	0.53	210	0.01	0.167	0.79	0.42	2.24	3.39	2.91	0.86
Average	0.92											
Co.V	12%											
PL-FRP-01	1200	1.2	0.53	210	0.01	0.167	0.79	0.42	4.10	5.36	5.05	0.94
PL-FRP-02	1200	1.2	0.53	210	0.01	0.167	0.79	0.42	4.10	5.36	5.81	1.08
PL-LIQ-01	1200	1.2	0.53	210	0.01	0.167	0.79	0.42	4.10	5.36	4.71	0.88
PL-LIQ-02	1200	1.2	0.53	210	0.01	0.167	0.79	0.42	4.10	5.36	4.38	0.82
PL-MYL-01	1200	1.2	0.53	210	0.01	0.167	0.79	0.42	4.10	5.36	6.12	1.14
PL-MYL-02	1200	1.2	0.53	210	0.01	0.167	0.79	0.42	4.10	5.36	5.11	0.95
Average	0.97											
Co.V	13%											

column with a separation film before the application of the FRP jacket. In this case, *Mylar*<sup>TM</sup> sheets were successfully used. They were applied on specimens in forms of half-scale columns made both by blocks of limestone and by blocks of Neapolitan tuff. The specimens were subjected to centered compression tests in order to evaluate the mechanical effectiveness of confinement for each of the solutions adopted. It was possible to appreciate that confinement is effective both in terms of increasing strength and ductility, regardless of the solution adopted for the application of the reinforcement. Furthermore, at the conclusion of the tests conducted, it was possible to remove the C-FRP jackets from the masonry specimens and by comparing them it was possible to evaluate the degree of reversibility according to the installation technique adopted. Also in this sense, the results can be considered satisfactory. In fact, the concept of reversibility, as intended above, was not respected for the classical wet lay-up technique, due to the direct contact between the FRP jacket and the masonry core. Therefore, the total restoration of the original conditions resulted impossible since the removal of the FRP jacket involves the removal of the substrate on which the C-FRP system is bonded. It should also be noted that the removability of the intervention cannot be

achieved even by heating the resin, due to its thermosetting behavior. When an innovative technique is applied, as those proposed herein, it resulted possible to remove the C-FRP jacket, without changing the aspect of the masonry substrate and the surface of the column.

In particular, those samples previously treated with adhesion inhibiting products (LAI technique), suffered a modest surface alteration when compared with those samples confined without any liquid treatment and subjected to the same confinement and rupture cycle. These results take on greater prominence and encourage a continuation of the experimentation on the use of adhesion inhibitors with a view to reversibility of the interventions with FRP on natural stones, if we consider that Lecce and Neapolitan tuff, tested herein, result very porous materials. If the same technique would be used to natural stones with lower porosity, the proposed technique would certainly guarantee a higher reversibility and absence of color alteration, respect to the case shown in this study. A possible development of the field of experimentation would be to test further combinations and dosages of the materials that inhibit adhesion, or to add the inhibitory liquid with thickness so as to make it sufficiently viscous and allow it, upon drying, to create



a patina of surface able to avoid resin penetration inside the stone.

If the LAI technique is promising in order to make the confinement of the masonry columns with the FRPs reversible, the ISF technique, provided satisfactory results under all aspects. In fact, wrapping the masonry columns with *Mylar*<sup>TM</sup> sheets, before applying the FRP jacket, allows to completely remove it after the tests, safeguarding the physical and chromatic integrity of the masonry substrate, even also when frescos could be present on the surface. In this case, therefore, the reinforcement was not only removable but also reversible. The technique in this context was applied for the continuous wrapping, but the proposed solution is also valid when discontinuous FRP strips are planned in the design provisions.

In summary, the results of the experimentation constitute an excellent starting point in identifying new FRP-confinement techniques to ensure the total reversibility of strengthening interventions with FRP in heritage masonry columns. With regard to the confinement technique after applying adhesion inhibiting liquids, the most suitable dosages relating to the inhibitory layers to prevent saturation of the stone remain to be defined in function of the masonry porosity and/or in the eventuality of plastered surface (like the before mentioned frescoed) where ISF should be preferred with respect to LAI in absence of proper experimental evidence. Lastly, the rounding of the corners is not always anymore forbidden, but it might be in some cases, especially if frescoed valuable surfaces are concerned, so it would be useful to foresee tests on multi-ply confinements without rounding to check the influence of the knife-effect and the effectiveness of the proposed solution also in these cases.

**Funding** Open access funding provided by Università della Calabria within the CRUI-CARE Agreement. The research presented in this article was funded by the Italian Ministry of University and Research in the framework of the national project PRIN (Progetti di ricerca di Rilevante Interesse Nazionale, 2017)—Project PRIN SURMOUNT “*Innovativesystemsbased oninorganicmortarandnon-metallicreinforcementforthe upgradeofmasonrystructuresandnon-structuralelements*”.

#### Declarations

**Conflict of interest** The authors have no competing interests to declare that are relevant to the content of this article.

**Open Access** This article is licensed under a Creative Commons Attribution 4.0 International License, which permits use, sharing, adaptation, distribution and reproduction in any medium or format, as long as you give appropriate credit to the original author(s) and the source, provide a link to the Creative Commons licence, and indicate if changes were made. The images or other third party material in this article are included in the article’s Creative Commons licence, unless indicated otherwise in a credit line to the material. If material is not included in the article’s Creative Commons licence and your intended use is not permitted by statutory regulation or exceeds the permitted use, you will need to obtain permission directly from the copyright holder. To view a copy of this licence, visit <http://creativecommons.org/licenses/by/4.0/>.

#### References

1. Parisi F, Augenti N (2013) Earthquake damages to cultural heritage constructions and simplified assessment of artworks. *Eng Fail Anal* 34:735–760
2. ISTAT «Censimento generale della Popolazione e delle Abitazioni» 9 Ottobre 2011. [Online]. Available: [http://dati-censimentopopolazione.istat.it/Index.aspx?DataSetCode=DICA\\_EDIFICIRES#](http://dati-censimentopopolazione.istat.it/Index.aspx?DataSetCode=DICA_EDIFICIRES#). [Accessed on Mar 2022]
3. Ministero delle Infrastrutture e dei Trasporti (2018) Nuove norme sismiche per il calcolo strutturale. Ministero delle Infrastrutture e dei Trasporti, Decreto Ministeriale del 17/01/2018. [In Italian]
4. Council of Europe recommendation of 1993 “On the protection of the architectural heritage against “natural disasters”, and especially the recommendation of the 1988 Skopje workshop
5. Rodwell D (2012) The UNESCO world heritage convention, 1972–2012: reflections and directions. *Hist Environ Policy Pract* 3(1):64–85
6. Borri A, Corradi M (2019) Architectural heritage: a discussion on conservation and safety. *Heritage* 2(1):631–647
7. Roca P (2011) Restoration of historic buildings: conservation principles and structural assessment. *Int J Mater Struct Integrity* 5(2–3):151–167
8. Coisson E, Ottoni F (2014) The use of composites in architectural restoration: some critical considerations on the theoretical implications. *Key Eng Mater* 624:11–18
9. Eurocode no 8 ‘Design provisions for earthquake resistance of structures’
10. ICOMOS (2003) Charter—principles for the analysis, conservation and structural restoration of architectural heritage
11. ISO 13822 (2010) Bases for design of structures—assessment of existing structures. Technical committee: ISO/TC 98/SC 2. Publication date: 2010–08
12. Linee Guida per la valutazione e riduzione del rischio sismico del patrimonio culturale (Guidelines for evaluation and mitigation of seismic risk to cultural heritage), 2010. [In Italian]
13. Masia MJ, Shrive NG (2003) CFRP wrapping for the rehabilitation of masonry columns. *Can J Civil Eng* 30:734–744. <https://doi.org/10.1139/l03-015>
14. Faella C, Martinelli E, Paciello S, and Nigro E (2004) “Experimental tests and theoretical models on tuff masonry bricks and columns confined with C-FRP sheets”. In



- Proceedings of IMTCR04 international conference, Vol. 2, A. Nanni and A. La Tegola eds., pp. 343–359
15. Kreaikas TD, Triantafyllou TC (2005) Masonry confinement with fiber-reinforced polymers. *J Compos Constr* 9:128–135. [https://doi.org/10.1061/\(ASCE\)1090-0268\(2005\)9:2\(128\)](https://doi.org/10.1061/(ASCE)1090-0268(2005)9:2(128))
  16. Aiello MA, Micelli F, Valente L (2007) Structural upgrading of masonry columns by using composite reinforcements. *J Compos Constr* 11(6):650–658
  17. D'Ambra C, Di Ludovico M, Balsamo A, Prota A, and Manfredi G (2008) "Confinement of tuff and brick masonry columns with FRP laminates". In: Proceedings of the 3rd conference on mechanics of masonry structures strengthened with composite materials- MURICO 3 (Venice), 232–240
  18. Aiello MA, Micelli F, Valente L (2009) FRP confinement of square masonry columns. *J Compos Constr* 13(2):148–158
  19. Micelli F, Di Ludovico M, Balsamo A, Manfredi G (2014) Mechanical behaviour of FRP-confined masonry by testing of full-scale columns. *Mater Struct* 47:2081–2100
  20. Micelli F, Angiuli R, Corvaglia P, Aiello MA (2014) Passive and SMA-activated confinement of circular masonry columns with basalt and glass fibers composites. *Compos B Eng* 67:348–362
  21. Minafò G, Monaco A, D'Anna J, La Mendola L (2018) Compressive behaviour of eccentrically loaded slender masonry columns confined by FRP. *Eng Struct* 172:214–227. <https://doi.org/10.1016/j.engstruct.2018.06.011>
  22. Sandoli A, Ferracuti B, Calderoni B (2019) FRP-confined tuff masonry columns: regular and irregular stone arrangement. *Compos B Eng* 162:621–630
  23. Cascardi A, Lerna M, Micelli F, Aiello MA (2020) Discontinuous FRP-confinement of masonry columns. *Front Built Environ* 5:147
  24. Alotaibi KS, Islam AS, Galal K (2022) Axial performance of grouted C-shaped concrete block masonry columns jacketed by carbon and glass FRP. *Eng Struct* 267:114698
  25. Estevan L, Baeza FJ, Maciá A, Ivorra S (2022) FRP confinement of stone specimens subjected to moisture and preload. *Int J Archit Herit* 16(1):19–32
  26. Agante M A, Júlio E, Barros J A, & Santos J (2017) Active CFRP-based confinement strategies for RC columns with rectangular cross sections. In: 5th international specialty conference in fibre reinforced materials at: Singapore
  27. Lignola GP, Angiuli R, Prota A, Aiello MA (2014) FRP confinement of masonry: analytical modeling. *Mater Struct* 47:2101–2115
  28. Rao KSN, Pavan GS (2015) FRP-confined clay brick masonry assemblages under axial compression: experimental and analytical investigations. *J Compos Constr* 19(4):04014068. [https://doi.org/10.1061/\(asce\)cc.1943-5614.0000525](https://doi.org/10.1061/(asce)cc.1943-5614.0000525)
  29. Cascardi A, Dell'Anna R, Micelli F, Lionetto F, Aiello MA, Maffezzoli A (2019) Reversible techniques for FRP-confinement of masonry columns. *Constr Build Mater* 225:415–428
  30. CNR-DT 200 R1/2013 (2013) Guide for the design and construction of externally bonded FRP systems for strengthening existing structures, national research council, Rome

**Publisher's Note** Springer Nature remains neutral with regard to jurisdictional claims in published maps and institutional affiliations.

